Novel Sulfonated Polyimide Ionomers by Incorporating Pyridine Functional Group in the Polymer Backbone

Rui Lei,[1,2] Chuanqing Kang,[1,2] Yunjie Huang,[1,2] Yuhan Li,[1,2] Xi Wang,[1,2] Rizhe Jin,[1] Xuepeng Qiu,[1] Xiangling Ji,[1] Wei Xing,[1] Lianxun Gao[1]

[1]*State Key Laboratory of Polymer Physics and Chemistry, Changchun Institute of Applied Chemistry, Chinese Academy of Sciences, Changchun 130022, People's Republic of China*
[2]*Graduate School of the Chinese Academy of Sciences, Beijing 100049, People's Republic of China*

Received 24 March 2009; accepted 10 June 2009
DOI 10.1002/app.30929
Published online 28 July 2009 in Wiley InterScience (www.interscience.wiley.com).

ABSTRACT: A series of sulfonated polyimides (SPIs) containing pyridine ring in the polymer backbone were synthesized by the polycondensation of 1,4,5,8-naphthalene-tetracarboxylic dianhydride (NTDA), 5-(2,6-bis(4-aminophenyl)pyridin-4-yl)-2-methoxy benzene sulfonic acid (SDAM), and 4,4′-diaminodiphenyl ether (ODA). Flexible, transparent, and tough membranes were obtained. Property study revealed that all the membranes displayed high thermal stability with the desulfonation and decomposition temperature higher than 290 and 540°C, respectively, as well as good mechanical property with Young's modulus larger than 1.0 GPa, maximum strength (MS) on a scale of 60–80 MPa, and elongation at break (EB) ranged from 41.79 to 75.17%. More importantly, the new materials exhibited small water uptake and excellent dimensional stability with the highest sulfonated SPI-80 showing the maximum water uptake of 36.1%, and maximum swollen ratio of $\Delta t = 0.038$ and $\Delta l = 0.026$, respectively (Δt and Δl stands for the thickness and diameter change of the film, respectively). The high water stability exhibited by the SPI films is attributed to the formation of inner salts and/or ionic crosslinking between the sulfonic acid and pyridine functional groups, which suppresses the water uptake ability of sulfonic acid and strengthened the interpolymer chain interactions. Thus, the excellent water stability, good thermal and mechanical properties, and the technologically applicable conductivity of SPI-80 render this material attractive for proton exchange membrane (PEM) application. © 2009 Wiley Periodicals, Inc. J Appl Polym Sci 114: 3190–3197, 2009

Key words: sulfonated polyimide; pyridine; acid–base interaction; water stability; proton conductivity

INTRODUCTION

Proton exchange membrane fuel cells (PEMFCs) have attracted considerable interests as a clean electrical power source for vehicles, stationary, and portable applications.[1–3] As a vital component of PEMFC, proton exchange membrane (PEM) plays a crucial role in fuel cells for conducting proton and separating gas. Practical application of a PEM requires the material possessing high proton conductivity, as well as high resistance against mechanical fatigue and chemical disruption. So far, a vast number of materials have been investigated, with perfluorinated Nafion[4] as the most successful example because of its good thermal and mechanical properties and high conductivity.[5] However, this material was not entirely satisfactory for the sake of its low proton conductivity at low humidity and/or high temperature (>80°C), high methanol permeability, and high cost. Therefore, the development of PEM materials with enhanced properties and low cost remains an important challenge.

Thus, recent investigations are shifted to the nonfluorinated materials with sulfonated polyimides (SPIs) and are of particular interest. This class of materials offers inherently several advantages over others, including excellent thermal and mechanical stability, superior chemical resistance, low methanol permeability, and so forth, rendering them attractive as PEM materials.[6–9] Thus, notable studies were focused on the development of SPI-based PEMs possessing not only high proton conductivity but also good water stability. One of the most popular strategies to this end is the structural modification of monomers, for instance, by introducing functional groups to form ionic or H-bonding interactions with sulfonic groups in the derived polymers.[10–13]

As an active group within the domain of polyimide materials,[14] we have previously investigated the SPIs derived from the copolymerization of

Correspondence to: L. Gao (lxgao@ciac.jl.cn).
Contract grant sponsor: Department of Science and Technology of Jilin Province; contract grant number: 20086019.
Contract grant sponsor: Ministry of Science and Technology of China; contract grant number: 2006AA03Z224.

1,4,5,8-naphthalene-tetracarboxylic dianhydride (NTDA), 4,4′-diaminodiphenyl ether (ODA), and naphthyl-contained diamine,[15] in which the structural nature of naphthyl motifs was shown to be important to influence the properties of the resulting PEMs by affecting the polymer microstructure for water holding. Consequently, the polymers displayed good proton conductivity, whereas the water stability was poor due to the excessive water uptake. To overcome this problem, we recently designed and synthesized a novel class of SPI copolymers of an otherwise identical structure, but replacing the naphthyl moieties of our previously reported polymers with 5-(2,6-bis(4-aminophenyl)pyridin-4-yl)-2-methoxy benzene sulfonic acid (SDAM). We proposed that by incorporating the pyridine ring in polymer backbone, the strong intra and/or inter acid–base interactions would be formed between the sulfonic acid and pyridine functional groups to compare with the frequently reported weak H-bonding interactions, thereby suppressing membrane swelling. Herein, we present the synthesis of monomer SDAM and the corresponding SPI copolymers, and the study on the properties of various membranes.

EXPERIMENTAL SECTION

Materials

NTDA was purchased from Aldrich Chemical and purified by vacuum sublimation. All other reagents were purchased from Shanghai Chemical Reagent Plant (Shanghai, China). Triethylamine (TEA) was dried over sodium followed by distillation. *m*-Cresol was purified by distillation under reduced pressure. Other reagents were of analytical grade and used as received.

Synthesis of 5-(2,6-bis(4-nitrophenyl)pyridin-4-yl)-2-methoxybenzenesulfonic acid

To a 100-mL three-necked flask equipped with a mechanical stirring device, 15 mL of concentrated (95%) sulfuric acid was charged. 4-(4-Methoxy)phenyl-2,6-bis(4-nitrophenyl)pyridine (DNM; 4.27 g, 0.10 mol), which was synthesized according to the reported methods,[16] was added slowly under stirring after the reaction vessel was cooled to 0°C with an ice bath. The resulting solution was stirred at 0°C for 1 h and then heated at 60°C for 4 h. After being cooled to room temperature, the slurry mixture was carefully poured into 50% cold ethanol. The yellow solid thus formed was collected by filtration and washed with acetone thoroughly, and then dried under vacuum at 80°C to give the desired product (5.30 g, 93%). ^{1}H-NMR (400 MHz, DMSO-d_6): δ = 8.60 (d, 4 H, J = 8.8 Hz), 8.38 (d, 4 H, J = 8.8 Hz), 8.34 (s, 2 H), 8.29 (d, 1 H, J = 2.4 Hz), 8.09 (dd, 1 H, J = 8.6, 2.4 Hz), 7.19 (d, 1 H, J = 8.6 Hz), 3.89 (s, 3 H). FTIR (KBr, cm^{-1}): 2845, 1594, 1548, 1518, 1349, 1292, 1259, 1188, 1139, 1107, 1082, 854, 821.

Synthesis of 5-(2,6-bis(4-aminophenyl)pyridin-4-yl)-2-methoxy benzene sulfonic acid

To a 500-mL three-necked round-bottomed flask, equipped with a reflux condenser and a dropping funnel, 5-(2,6-bis(4-nitrophenyl)pyridin-4-yl)-2-methoxybenzenesulfonic acid (SDNM; 6.08 g, 0.012 mol), 5% palladium on carbon (0.4 g), and ethanol (200 mL) were charged. Then, 80% hydrazine hydrate (10 mL) in water (50 mL) was added dropwise through the funnel over a 1.5 h period under nitrogen atmosphere. The reaction mixture was then refluxed for 2 h and the hot solution was filtered to remove the palladium catalyst. The white cream-colored crystals formed upon cooling was collected by filtration. The crude product was repurified by precipitating out from the concentrated hydrochloric acid solution by slow addition of deionized water. The precipitate thus formed was collected by filtration, washed with acetone carefully, and then dried at 80°C *in vacuo* to give the pure product (2.51 g, 46%). mp: 288–289°C. ^{1}H-NMR (400 MHz, DMSO-d_6): δ = 8.25 (s, 1 H), 8.06 (d, 1 H, J = 8.8 Hz), 8.01 (d, 4 H, J = 7.2 Hz), 7.92 (s, 2 H), 7.16 (d, 1 H, J = 8.8 Hz), 6.93 (d, 4 H, J = 7.2 Hz), 3.86 (s, 3 H). FTIR (KBr, cm^{-1}): 3351, 2845, 2592, 1597, 1501, 1293, 1248, 1187, 1081, 822, 718. Elemental analysis: Calculated for $C_{24}H_{21}N_3O_4S$: C, 64.43%; H, 4.70%; N, 9.40%. Calculated for water content of 7.45 wt % in the sample: C, 59.63%; H, 5.18%; N, 8.70%. Found: C, 59.66%; H, 5.05%; N, 8.84%.

Synthesis of random NTDA-SDAM-ODA copolyimides

Taking the synthesis of SPI-50 as a typical example, to a 50-mL well-dried three-necked flask, NTDA (0.5360 g, 2 mmol), SDAM (0.4470 g, 1 mmol), ODA (0.2002 g, 1 mmol), benzoic acid (0.5190 g, 4.25 mmol), TEA (0.31 mL), and *m*-cresol (6.0 mL) were added. The mixture was stirred at room temperature for a few minutes, and then stirred at 80°C for 4 h and 180°C for 8 h under nitrogen flow, respectively. The resulting solution was poured into acetone after being cooled to 80°C. The fiber-like precipitate thus formed was collected by filtration and washed with acetone. The crude product was further purified by Soxhlet extraction with ethanol for 24 h and dried in vacuum at 120°C for 12 h.

Synthesis of model compounds

Synthesis of model compound-1

To a 250-mL three-necked flask, equipped with a reflux condenser, 4-(4-Methoxy)phenyl-2,6-bis(4-

aminophenyl)pyridine (DAM, 1.84 g, 5 mmol), which was prepared according to the known methods,[16] phthalic anhydride (1.63 g, 11 mmol), and 100 mL acetic acid were charged. The mixture was refluxed for 10 h under stirring. Then the yellow precipitate was collected by filtration, washed with water carefully, and dried at 100°C *in vacuo* to give the model compound-1 (MD-1; 2.80 g, 89%). ^{1}H-NMR (400 MHz, DMSO-d_6): δ = 8.50 (d, 4 H, J = 8.6 Hz), 8.28 (s, 2 H), 8.08 (d, 2 H, J = 8.8 Hz), 8.01 (m, 4 H), 7.94 (m, 4 H), 7.65 (d, 4 H, J = 8.6 Hz), 7.14 (d, 2 H, J = 8.8 Hz), 3.87 (s, 3 H).

Preparation of model salt (MD-2) for FTIR analysis

To a 50-mL three-necked flask, MD-1 (1.25 g, 2 mmol), *p*-toluenesulfonic acid (PTSA) monohydrate (1.14 g, 6 mmol), and 5 mL THF were added. Then, the mixture was stirred for a few minutes at room temperature, the resulting yellow solid was collected by filtration, washed with THF thoroughly and dried at 80°C *in vacuo* to give the model compound-2 (MD-1+PTSA).

Membrane formation and proton exchange

Films (in TEA salt form) were prepared by casting the *m*-cresol solution (5 wt %) on the glass plate and dried at 80°C for 48 h. The membranes were soaked in alcohol at room temperature for 10 h to remove the residual solvent. The proton-exchange treatment was carried out in 1 mol/L H_2SO_4 solution at room temperature, and the completion of proton exchange was confirmed by the disappearance of the peaks corresponding to the TEA salt in the Fourier transform infrared (FTIR) spectra of the membranes, and then the proton form films were washed with deionized water thoroughly.

Characterization of membranes

Measurements

FTIR spectra were determined with a Bio-Red Digilab Division FTS-80 spectrometer. ^{1}H NMR spectra were recorded on a Varian Unity spectrometer at 400 Hz with tetramethylsilane as an internal standard. Thermogravimetric analyses (TGA) were obtained at a heating rate of 10°C/min in nitrogen atmosphere with a Perkin–Elmer TGA-2 thermogravimetric analyzer. The tensile measurements were carried out on an Instron model 1122 at room temperature. Inherent viscosities were determined at 30°C with an Ubbelodhe viscometer in 0.5 g/dL *m*-cresol solution.

Ionic-exchange capacity

The ionic-exchange capacity (IEC) was measured by means of a classical titration method. A membrane sample (ca. 100 mg) was soaked in 100 mL saturated NaCl solution for 2 days. The released protons were titrated using a 0.01 mol/L NaOH solution.

Proton conductivity

Proton conductivity was measured using an electrochemical impedance spectroscopy technique (Model 5210 Frequency Response Detector, EG&GPARC, Princeton, NJ) over the frequency ranging from 0.1 Hz to 1 MHz. A four-point-probe cell with two pairs of platinum plate electrodes pressed with a sample membrane was mounted in a sealed Teflon cell. The distance between two electrodes was 1 cm. The cell was placed in a thermocontrolled chamber in deionized water for measurement. The resistance value associated with the membrane conductivity was determined from high-frequency intercept of the impendence with the real axis. Proton conductivity (σ) was calculated from eq. (1):

$$\sigma = L/(RS) \tag{1}$$

where σ, L, R, and S denote the proton conductivity, thickness of membranes (100% RH), the resistance of the membrane, and the cross-sectional area of the membrane, respectively.

Water uptake and dimensional change

The membranes were first dried in a vacuum oven at 100°C for 12 h. Then the water absorption experiments were carried out by immersing three sheets of films (ca. 100 mg per sheet) of each polyimide in water at the given temperature for 5 h. Then the films were taken out, wiped with tissue paper and quickly weighed on a microbalance. Water uptake (S) was calculated from eq. (2):

$$S = (W_s - W_d)/W_d \times 100\% \tag{2}$$

where W_d and W_s are the weights of dry and corresponding water-swollen film sheets, respectively.

Dimensional change was measured by immersing the round-shaped samples into deionized water at 80°C for 5 h. The changes of thickness and diameter were calculated from eq. (3):

$$\Delta t = (t - t_s)/t_s \qquad \Delta l = (l - l_s)/l_s \tag{3}$$

where t_s and t are the thickness, and l_s and l are the diameter of the membrane before and after soaking treatment, respectively.

Methanol permeability measurement

Methanol permeability of membranes was measured using a liquid permeation cell composed of two

compartments, which were separated by a vertical membrane. The membrane was first immersed in water to get the water-swollen sample and then set into the measurement cell (effective area: 3.8 cm^2). One compartment of the cell (V_1) was filled with methanol feed solution, and the other compartment (V_2) was filled with distilled water. Methanol permeates across the membrane by the concentration difference between the two compartments. The compartments were stirred continuously during the permeability measurement. The methanol concentration in the receiving compartment as a function of time is given by:

$$C_{2(t)} = AP_MC_1(t - t_0)/V_2L \quad (4)$$

where P_M is the methanol permeability, A and L are the area and thickness of the swollen membrane, respectively; C_1 and C_2 are the initial and permeated methanol concentration, respectively; t_0 and t correspond to the time when C_1 and C_2 were measured, respectively. There is a linear relationship between a series of C_2 and their corresponding measure-time t. Thus, methanol permeability (P_M) can be calculated from the following equation:

$$P_M = V_2Lk/AC_1 \quad (5)$$

where k is the slope of the straight line. The methanol concentration was measured by using a gas chromatography equipped with a thermal conductivity detector (Shimadzu, GC-2010A, Tokyo, Japan).

RESULTS AND DISCUSSION

Synthesis and characterization of the monomer and polyimides

Synthesis of monomer SDAM is outlined in Scheme 1. DNM was synthesized using a modified Chichibabin reaction according to the reported method.[16] Sulfonation of DNM with concentrated sulfuric acid at 60°C afforded SDNM. It should be noted that sulfonation at a higher temperature proved futile, producing intractable mixtures. Reduction of nitro group in SDNM with hydrazine hydrate catalyzed by 5 wt % Pd on carbon delivered the SDAM. The structures of the desired product were determined by ^{1}H-NMR and IR spectroscopic techniques.

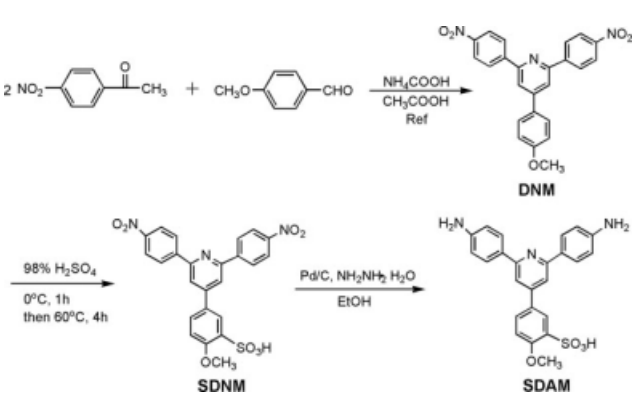

Scheme 1 Synthesis of the diamine monomer SDAM.

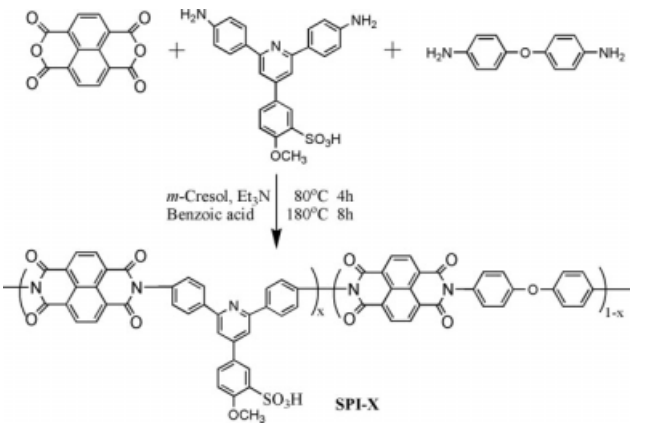

Scheme 2 Synthesis of SPI-*X* (*X* is the molar ratio of sulfonated diamine SDAM).

The preparation of SPIs was carried out by a one-pot polycondensation of dianhydride and diamines in the presence of TEA and benzoic acid (Scheme 2). Various SPI-*X* were synthesized by controlling the feeding ratio of SDAM to ODA, where *X* indicates the molar percentage of SDAM and increased gradually from 40, 50, 60, 70, 80, to 100%. The structures of the derived TEA-free films were characterized by FTIR spectrometry. Figure 1 shows the IR spectrum of SPI-80 as a representative example (only zoomed region from 500 to 2000 cm^{-1} was shown for clarity).

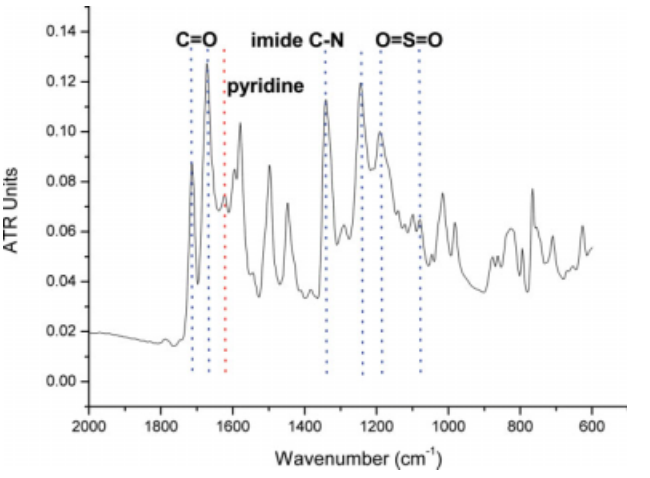

Figure 1 FTIR spectrum of SPI-80 (proton form). [Color figure can be viewed in the online issue, which is available at www.interscience.wiley.com.]

TABLE I
Inherent Viscosity and Solubility Behaviors of SPI-X (Et_3N Form)

SPI-*X*	Inherent viscosity (dL/g)	Solvents				
		m-Cresol	DMAC	DMSO	NMP	DMF
SPI-40	1.10	+	+	+	+	+
SPI-50	1.12	+	+	+	+	+
SPI-60	1.26	+	+	+	+	+
SPI-70	1.25	+	+	+	+	+
SPI-80	1.09	+	+	+	+	+
SPI-100	1.60	+	+	+	+	+

Note: +, soluble at room temperature; *X*, the molar ratio of sulfonated diamine (SDAM).

The peaks at 1714, 1672, and 1341 cm^{-1} are assigned to the carbonyl and C—N vibrations of naphthalenic imides, respectively. The absorption band appeared at 1623 cm^{-1} is the characteristic one of pyridine ring, and the band that appeared at 1245 cm^{-1} represents the vibration of the ether bond for connecting the two phenylene rings. Finally, two bands at 1191 and 1080 cm^{-1} are the typical stretch vibration of sulfonic acid group. It should be mentioned that for SPI-100 only fragile films were obtained from several SPI-100s with different inherent viscosities (1.45–1.60 dL/g in *m*-cresol), which makes it difficult to determine the structure and measure the properties of SPI-100.

Table I shows the viscosities and the solubilities of various resulting polymers as Et_3N form. The polymers had inherent viscosities ranging from 1.09 to 1.26 dL/g in *m*-cresol, which is indicative of high-molecular-weight polymers. In general, the polymers displayed good solubility in a broad range of polar solvents such as *m*-cresol, *N*,*N*-dimethylacetamide (DMAc), *N*,*N*-dimethyl formamide (DMF), dimethyl sulfoxide (DMSO), and *N*-methyl-2-pyrrolidinone (NMP) at room temperature.

Thermal stability and mechanical properties

Thermal stability of the SPIs was investigated by TGA analysis. Figure 2 depicts the TGA curve of SPI-70 as a representative example. The onset weight loss for SPI-70 around 100°C is due to the adsorbed water in the sample. The second and third loss stages at ca. 290 and 572°C correspond to the desulfonation of the sulfonic acid groups and the decomposition of the polymer main chain, respectively. The weight loss behaviors of SPI-40, 50, 60, and 80 are very similar to that of SPI-70 (data not shown), showing in general a desulfonation temperature at ca. 290°C and degradation temperature higher than 545°C. The data are evident that SPIs presented here exhibited good thermal stability.

The mechanical properties of the SPIs are summarized in Table III as indicated by the 0-h soaking time. The results showed that, in general, these materials displayed good mechanical properties with Young's modulus (YM) larger than 1.0 GPa, maximum strength (MS) on a scale of 60–80 MPa, and elongation at break (EB) ranging from 37.2 to 75.17%.

Water uptake, dimensional change, and IEC

Water uptake is a key parameter when practical application of a PEM is under consideration. The water within a membrane is necessary for carrying protons, however, excessive water uptake may result in the exorbitant dimensional change as well as the loss of mechanical strength of the film. Figure 3 depicts the water uptake of various SPI membranes with different degrees of sulfonation (DS) as a function of temperature. Clearly, the water uptake of the SPIs depends on the DS with higher sulfonated materials exhibit increased water uptake. Such

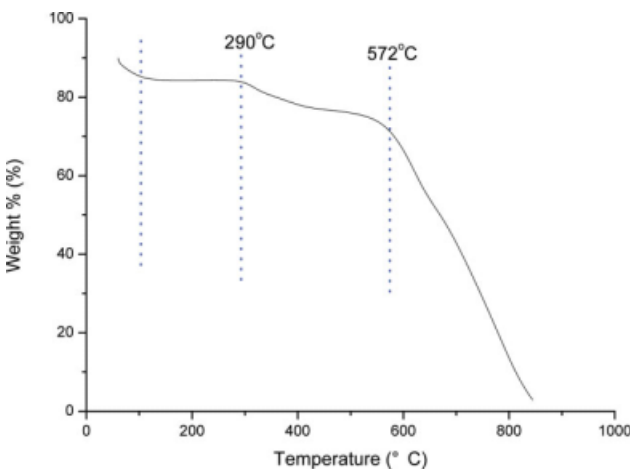

Figure 2 TGA curve for SPI-70 (proton form). [Color figure can be viewed in the online issue, which is available at www.interscience.wiley.com.]

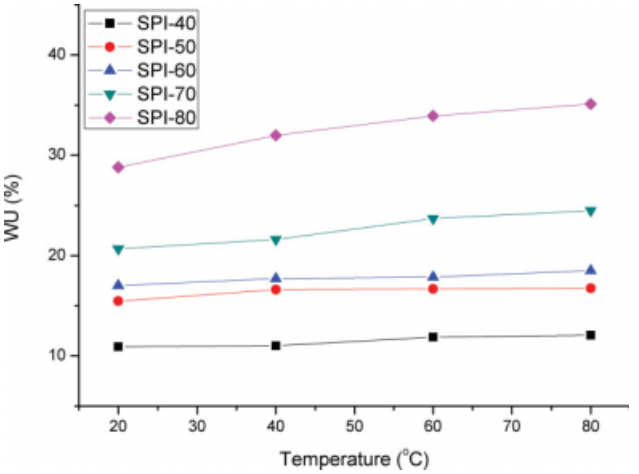

Figure 3 Water uptake of SPI-*X* membranes at different temperature. [Color figure can be viewed in the online issue, which is available at www.interscience.wiley.com.]

tendency is in agreement with many reported examples.[8] However, an impressive observation for our SPIs is that they showed a much lower water uptake than those appeared in literatures.[15,17] As can be seen from Figure 3, the water uptake is lower than 20% at 80°C for SPI-40, 50, and 60, and is ca. 36.1% even for the highest sulfonated SPI-80.

Table III lists the dimensional change of the SPIs. The data showed that all the SPIs exhibit very small dimensional change, with the maximum $\Delta t = 0.038$ and $\Delta l = 0.026$, where Δt and Δl stand for the thickness and length change of the film after and before soaking, respectively. The results are somewhat better than the NTDA-based analog SPIs presented in the literature, where Δt and Δl were in a range from 0.11–0.58 to 0.01–0.079, respectively.[18,19]

As for the IEC, we observed that while both the theoretical and experimental values increased gradually with the increase of DS, the experimental value was generally much smaller than the corresponding calculated ones (Table III). This observation is in sharp contrast to the frequently reported materials, where the calculated and experimental data were almost identical.[20] We proposed that the reduced experimental IEC, the low water uptake, and the small dimensional change exhibited by these SPIs are attributed probably to the strong intra and inter acid–base interactions between the pyridine and sulfonic acid, which reduces the water holding ability

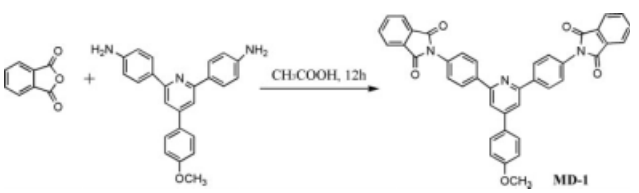

Scheme 3 Synthesis of model compound-1.

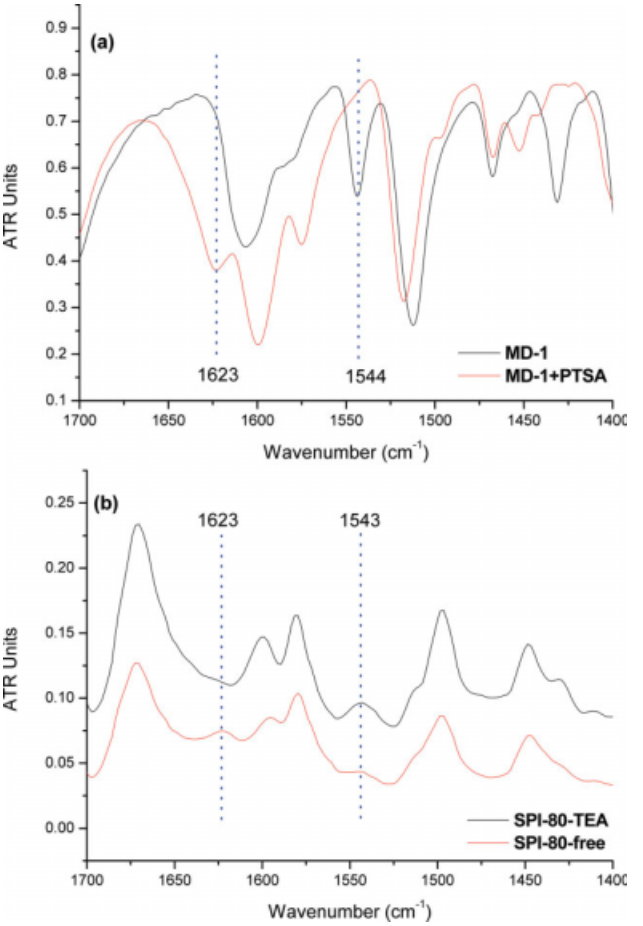

Figure 4 FTIR spectrum in the regions 1700–1400 cm^{-1} of (a) model compounds and (b) SPI-80. [Color figure can be viewed in the online issue, which is available at www.interscience.wiley.com.]

of sulfonic acid group, and ultimately, displaying low water uptake, small swollen ratio, and lower measured IECs than calculated ones.

To further examine our assumption, we carried out control experiments with the nonsulfonated MD-1 as the reference compound (Scheme 3). Figure 4(a)

TABLE II
Mechanical Properties and Weight Loss of the Resulting Membranes Before and After Aging in Boiling Water

SPI-*X*	Soaking time (h)	Weight loss (wt %)	MS (MPa)	YM (GPa)	EB (%)
SPI-40	0		69.54	1.48	69.76
	48	3.15	41.90	1.40	29.72
SPI-50	0		69.41	1.37	37.20
	48	3.72	61.61	1.36	24.40
SPI-60	0		74.41	1.43	54.88
	48	3.77	57.87	1.49	22.65
SPI-70	0		72.96	1.07	75.17
	48	3.93	67.52	1.05	22.87
SPI-80	0		72.48	1.25	49.51
	48	4.00	62.63	1.30	25.73

TABLE III
IEC, Dimensional Change, and Water and Oxidative Stability of SPI Membranes at 80°C

	Dimensional change		IEC (mequiv/g)			
SPI-*X*	Δt_c	Δl_c	Theoretical	Experimental	Water stability (h)	Oxiditive stability (h)
SPI-40	0.007	0.017	0.826	0.313	>1000	20
SPI-50	0.021	0.017	0.968	0.345	>1000	16
SPI-60	0.019	0.022	1.093	0.434	>1000	16
SPI-70	0.037	0.028	1.204	0.487	>1000	12
SPI-80	0.038	0.026	1.303	0.864	>1000	10

illustrates the IR spectra of MD-1 before and after treated with PTSA. In the spectrum of free MD-1, a strong peak that appeared at 1544 cm^{-1} is assigned to the pyridine ring. However, this band disappears completely when MD-1 is treated with PTSA, and instead, a new peak at 1623 cm^{-1} emerges. This new peak is assigned to the protonated pyridine ring and indicates unambiguously the acid–base interactions between the pyridine and sulfonic acid. In fact, such an acid–base interaction is also observed for the SPIs when the IR spectra of the TEA and H-form of SPIs are compared. For instance, the TEA form of SPI-80 exhibits a strong peak at 1543 cm^{-1} in the IR spectrum corresponding to pyridine ring [Fig. 4(b)]. Interestingly, after the TEA form of SPI was exchanged to its H-form, an absorption band at 1623 cm^{-1} appears accompanied by a notable reduction of the peak at 1543 cm^{-1}. These results firmly confirmed that the acid–base interaction between the pyridine ring and sulfonic acid (SPI-SO_3H + Pyr → [SPI-SO_3]$^-$ [H-Pyr]$^+$) occurs in the SPIs, and this interaction should play an important role for the lowered water uptake, small swollen ratio, and the reduced IEC of the obtained SPI films.

Water and oxidative stability

To examine the water stability of our SPIs, we studied the properties of the SPIs after immersing the films in boiling water for 48 h. The results revealed that all the films maintained mechanical properties with weight loss $\leq$4.0%, YM > 1.0 GPa, MS > 41.90 MPa, and EB > 22%, respectively (Table II). Continuous boiling until at break as judged by slight bending the films revealed that the time could be extended to more than 300 h. We also investigated the water stability of the films at 80°C, and the results showed that all the SPI membranes are tough enough until immersing the films in water for more than 1000 h. As mentioned earlier, water stability of a membrane correlates closely with its water uptake, and generally, a PEM with low water uptake exhibits good stability against water disruption.[21] For our SPIs, we reasoned that in addition to the low water uptake, an additional effect due to the interchain acid–base interactions should be considered, which strengthens the mechanical properties of the derived films.

The oxidative stability of SPI ionomers was also investigated by measuring the lasting time of the films until at break by bending the films gently after immersing in Fenton's reagent (30 ppm $FeSO_4$ in 30% H_2O_2) at 80°C. As listed in Table III, the materials exhibit good resistance against HO· and HOO· oxidants, although the lasting time is reduced gradually from 20 to 10 h with the increased DS. This is understandable because the oxidants are often contaminated by a certain amount of water which affects more significantly the stability of a film with higher DS than that with lower DS.

Proton conductivities and methanol permeability

The proton conductivities (σ) of the SPI membranes under various temperatures are summarized in Table IV. We found that for the SPIs with DS lower than 70%, the proton conductivity was low within a range from 0.45 to 0.86 × 10^{-2} S/cm and increased slightly when the temperatures were elevated from 20 to 80°C. However, a rapid increase was observed for SPI-80, showing a consequential proton conductivity of up to 1.07 × 10^{-2} S/cm at 20°C and 1.88 × 10^{-2} S/cm at 80°C, which is larger than the boundary datum for technological application (σ = 1.0 × 10^{-2} S/cm).[22] The methanol permeabilities of the SPI membranes

TABLE IV
Proton Conductivity and Methanol Permeability of SPI-*X* Membranes

	Proton conductivity (σ) (×10^{-2} S/cm)				
SPI-*X*	20°C	40°C	60°C	80°C	P_M (10^{-7} cm^2/s)
SPI-40	0.49	0.56	0.65	0.66	1.56
SPI-50	0.45	0.58	0.70	0.86	2.11
SPI-60	0.46	0.67	0.74	0.76	2.15
SPI-70	0.48	0.68	0.85	0.86	3.51
SPI-80	1.07	1.31	1.57	1.88	5.86

are listed in Table IV. Data show that the SPI films exhibit P_M within a range of $1.56-5.86 \times 10^{-7}$ cm^2/s at room temperature, which is about one order of magnitude lower than that of Nafion membranes (2.6×10^{-6} cm^2/s) at the same condition.

CONCLUSIONS

A series of SPIs with different degrees of sulfonation were prepared from the copolymerization of NTDA, SDAM, and ODA. Flexible, transparent, and tough membranes were obtained by solution casting, and these films displayed high thermal stability and good mechanical properties. Conceptually, by using SDAM as a component of the polymer, the pyridine ring incorporated in SDAM motif was proved to form a strong intra and/or inter acid–base interactions with the sulfonic acid. Such interaction is suggested to suppress membrane swelling. Consequently, the films prepared from this series of SPIs exhibited low water uptake and excellent water stability. In addition, the results presented here provide a useful strategy for the *de novo* design and fabrication of new PEM materials with enhanced performance. On the basis of this work, we are currently preparing other SPI-based materials toward the enhancement of the PEM properties.

References

1. Barbir, F.; G'omez, T. Int J Hydrogen Energy 1997, 22, 1027.
2. Savadogo, O. J N Mat Electrochem Syst 1998, 1, 47.
3. Carrette, L.; Friedrich, K. A.; Stimming, U. Fuel Cells 2001, 1, 1.
4. Sone, Y.; Ekdunge, P.; Simonsson, D. J Electrochem Soc 1996, 143, 1254.
5. Alberti, G.; Casciola, M. Solid State Ionics 2001, 145, 3.
6. Faure, S.; Mercier, R.; Aldebert, P.; Pineri, M.; Sillion, B. Fr. Pat 9,605,707 (1996).
7. Faure, S.; Cornet, N.; Gebel, G.; Mercier, R.; Pineri, M.; Sillion, B. In Proceedings of Second International Symposium on New Materials for Fuel Cell and Modern Battery Systems; Savadogo, O., Roberge, P., Eds.; École Polytechnique de Montréal: Montreal, Canada, 1997; p 818.
8. Roziere, J.; Jones, D. J. Annu Rev Mater Res 2003, 33, 503.
9. Hickner, M. A.; Ghassemi, H.; Kim, Y. S.; Einsla, B. R.; McGrath, J. E. Chem Rev 2004, 104, 4587.
10. Kerres, J.; Ullrich, A.; Meier, F.; Häring, T. Solid State Ionics 1999, 125, 243.
11. Kerres, J.; Ullrich, A. Sep Purif Technol 2001, 22, 1.
12. Yamada, M.; Honma, I. Electrochim Acta 2003, 48, 2411.
13. Hariharan, R.; Bhuvana, S.; Malbi, M. A.; Sarojadevi, M. J Appl Polym Sci 2004, 93, 1846.
14. Ding, M. X. Prog Polym Sci 2007, 32, 623.
15. Li, Y. H.; Jin, R. Z.; Wang, Z.; Cui, Z. M.; Xing, W.; Qiu, X. P.; Ji, X. L.; Gao, L. X. Polymer 2007, 48, 2280.
16. Tamami, B.; Yeganeh, H. Polymer 2001, 42, 415.
17. Watari, T.; Fang, J.; Tanaka, K.; Kita, H.; Okamoto, K.; Hirano, T. J Membr Sci 2004, 230, 111.
18. Yamada, O.; Yin, Y.; Tanaka, K.; Kita, H.; Okamoto, K. Electrochim Acta 2005, 50, 2655.
19. Yin, Y.; Yamada, O.; Suto, Y.; Mishima, T.; Tanaka, K.; Kita, K.; Okamoto, K. J Polym Sci Part A: Polym Chem 2005, 43, 1545.
20. Asano, N.; Aoki, M.; Suzuki, S.; Miyatake, K.; Uchida, H.; Watanabe, M. J Am Chem Soc 2006, 128, 1762.
21. Yin, Y.; Fang, J.; Watari, T.; Tanaka, K.; Kita, H.; Okamoto, K. J Mater Chem 2004, 14, 1062.
22. Liu, B.; Kim, D. S.; Murphy, J.; Robertson, G. P.; Guiver, M. D.; Mikhailenko, S.; Kaliaguine, S.; Sun, Y. M.; Liu, Y. L.; Lai, J. Y. J Membr Sci 2006, 280, 54.